Original Research Article

Salidroside Pre-Treatment Inhibits Hypertensive Renal Injury and Fibrosis Through Inhibiting Wnt/β-Catenin Pathway

Jie Zhu[1],*, Liang Li[1],*, Yuting Luan[2], Ziqing Zhang[1], Yi Wang[1], and Zhenyu Xu[1] ⬤

Abstract

Objectives: This study aimed to explore the protective effects and underlying mechanisms of salidroside (SAL) in angiotensin II (Ang II)-induced hypertensive renal injury and fibrosis, using in vivo and in vitro models.

Methods: In this study, we generated Ang II-induced hypertensive renal injury and fibrosis in mice and the recombinant interferon-gamma (IFN-γ)-stimulated murine podocyte clone 5 (MPC5) model in vitro. Histological and oxidative stress analyses were performed to evaluate the renal injury.

Results: SAL pre-treatment reduced systolic blood pressure (SBP), diastolic blood pressure (DBP), mean arterial blood pressure (MAP), and attenuated serum creatinine (Scr), blood urea nitrogen (BUN), and serum cystatin C (Cys-C) levels in Ang II-infused mice (all, $P < 0.001$). SAL reduced renal fibrosis and related molecules expression, including Collagen I, Collagen III, and α-smooth muscle actin (α-SMA) (all, $P < 0.001$). SAL decreased the content of malondialdehyde (MDA) while increasing superoxide dismutase (SOD), catalase (CAT), and glutathione peroxidase (GSH-Px) in Ang II-treated mice (all, $P < 0.001$). In addition, SAL pre-treatment inhibited AT1R, Wnt1, Wnt3a, and β-catenin expressions (all, $P < 0.001$), both in vivo *and* in vitro.

Conclusion: Our experimental data demonstrate that SAL pre-treatment protects against Ang II-induced hypertensive renal injury and fibrosis by suppressing the Wnt/β-catenin pathway in vivo and in vitro.

[1] Department of Emergency Medicine, Seventh People's Hospital of Shanghai University of Traditional Chinese Medicine, Shanghai, China
[2] Department of Infectious Diseases, Seventh People's Hospital of Shanghai University of Traditional Chinese Medicine, Shanghai, China

*Authors contributed equally.

Corresponding Authors:
Zhenyu Xu, Department of Emergency Medicine, Seventh People's Hospital of Shanghai University of Traditional Chinese Medicine, 358 Datong Road, Pudong, Shanghai 200137, China.
Email: Xzy2062@163.com

Yi Wang, Department of Emergency Medicine, Seventh People's Hospital of Shanghai University of Traditional Chinese Medicine, 358 Datong Road, Pudong, Shanghai 200137, China.
Email: 18017260669@189.cn

Introduction

Hypertensive renal injury is the leading cause of renal failure.[1] The primary cause of progressive hypertensive nephropathy (HN) is tubulointerstitial fibrosis.[2] The renin-angiotensin-aldosterone system (RAAS) regulates renal function and arterial pressure.[3] However, aldosterone and mineralocorticoid receptor (MR) activation are independent of the renin-angiotensin system (RAS) as the progression of chronic kidney disease (CKD) development.[4] Angiotensin II (Ang II), which is the primary effector of RAAS, can accelerate the progression of renal interstitial fibrosis by attenuating renal hemodynamics, controls the growth of endothelial cells (ECs) in the adult renal tubule, promotes the production of inflammatory and cellular cytokines, and increases the accumulation and degradation of the extracellular matrix (ECM) containing transforming growth factor beta 1 (TGFβ1), α-smooth muscle actin (α-SMA), fibronectin (FN) and collagen type I (Col-1).[5-8]

Currently, the primary treatment methods for HN focus on regulating blood pressure (BP) and protecting kidney function. RAAS inhibitors, such as angiotensin-converting enzyme (ACE) inhibitors and angiotensin receptor blockers (ARBs), are considered first-line treatments for hypertensive individuals with kidney disease. Although existing treatment methods can slow down the progression of hypertension, they have limited effectiveness in controlling hypertensive renal damage.[9] Therefore, exploring and developing the significant health effects of traditional Chinese medicine (TCM) is beneficial.

SAL (p-hydroxyphenethyl-β-D-glucoside), a phenylethanoid derivative, is the essential component isolated from *Rhodiola rosea L*. SAL is used in traditional medicine in various world regions, including Northern Europe, India, and China.[10,11] The chemical structure of SAL is represented in Figure 1(A). *Rhodiola rosea* L. has been found to have anti-fatigue, anti-hypoxia, anti-aging, and immunostimulatory effects, especially in extreme conditions such as high altitude with low oxygen levels, low temperatures, and increased atmospheric pressure.[12,13] The active ingredients of *Rhodiola rosea* L. primarily consist of phenyl alkyl glycosides, particularly salidroside (SAL).[14] SAL has been demonstrated in recent research to affect fibrosis in several organs significantly.[15-18] However, the molecular mechanisms by which SAL protects or reverses hypertensive renal injury and fibrosis are still unknown.

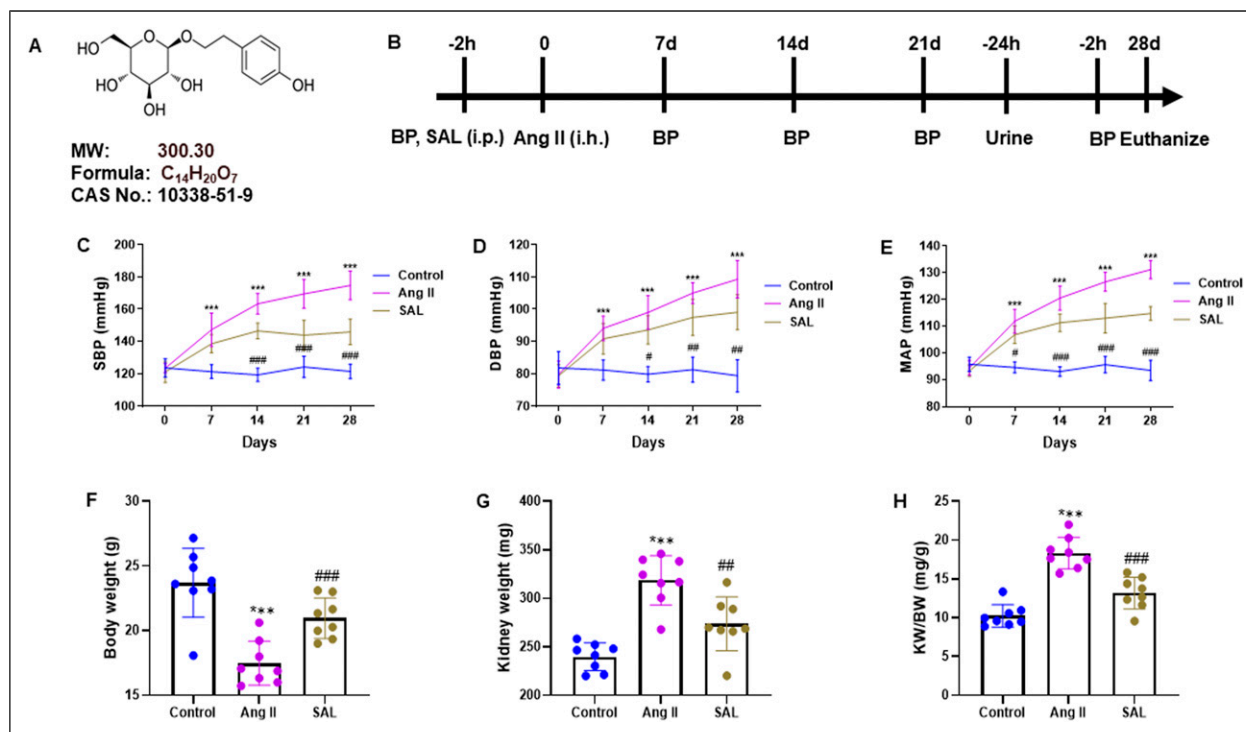The Wnt/β-catenin signaling pathway is a group of highly conserved signal transduction pathways in multicellular

Figure 1. SAL reduces blood pressure and renal hypertrophy index in Ang II-infused mice. (A) Chemical Structure, molecular weight, chemical formula and CAS number of SAL. (B) SAL was intraperitoneally injected (50 mg/kg/day) into mice 2 h before subcutaneous infusion of Ang II for 28 d. The timeline of the interventional procedure for SAL and Ang II is shown. (C, D, E) SAL reduced the SBP, DBP and MAP of Ang II-infused mice. SAL increased (F) body weight (BW) and decreased (G) kidney weight (KW) and (H) renal hypertrophy index (KW/BW) in mice with Ang II infusion. Data are presented as mean ± SD (n = 8 in each group) and analyzed using ANOVA. ***$P < 0.001$ vs control group; #$P < 0.05$, ###$P < 0.001$ vs Ang II group. SAL, salidroside; Ang II, angiotensin II; SBP, systolic blood pressure; DBP, diastolic blood pressure; MAP, mean arterial pressure.

organisms. It is critical in embryonic development and regulates several physiological functions in most organs, including cell survival, proliferation, inflammation, and fibrosis.[19] The Wnt/β-catenin signaling pathway is maintained in adult kidneys and under standard physiological settings by enhanced GS3K-dependent complex-caused β-catenin ubiquitination and proteasome destruction.[19-22] The Wnt/β-catenin signaling pathway is active in different types of kidney diseases, including acute kidney injury (AKI) (eg, ischemia and nephrotoxin) and chronic kidney injury (CKI) (eg, diabetes, Adriamycin, Ang II-induced nephropathy).[21,22] However, how the Wnt/β-catenin pathway affects Ang II-induced hypertensive renal injury and fibrosis is unclear. Therefore, we investigated the protective role of SAL on hypertensive renal injury and fibrosis and uncovered the precise molecular mechanism.

Material and Methods

Animals

Male C57BL/6 mice (8-10 weeks old) weighing 22-24 g were obtained from SLAC Laboratory Animal Co, Ltd (Beijing, China). They were kept in cages with unlimited access to food and water. All mice were kept in the SPF room at 20 °C–24 °C and 35%–45% humidity with a 12 h light/dark cycle. The animal study followed the Guide for the Care and Use of Laboratory Animals (NIH Publication No. 85-23, revised 1996), and our Hospital's Animal Care and Use Committee approved (2021-7th-HIRB-029) the study.

Mouse Model of Hypertensive Nephropathy

C57BL/6 mice (n = 24) were used to construct a hypertensive nephropathy model. All mice were divided into the Control, Ang II, and SAL groups. The mice were subcutaneously infused with Ang II (2.0 mg/kg/day) (Ang II and SAL groups) or the same volume saline (Control group) using osmotic mini-pumps for 28 consecutive days. Two hours before the start of Ang II infusion, the mice were intraperitoneally pre-injected with SAL (50 mg/kg/day, HY-N0109, MedChemExpress) (SAL group) or the same volume saline (Control and Ang II groups) once a day for 28 days. Figure 1(B) depicts the timeline of a mice interventional procedure.

Measurement of Blood Pressure

Systolic blood pressure (SBP) and diastolic blood pressure (DBP) were measured using the tail-cuff method (ALC-NIBP; Shanghai Alcott Biotech Co, Shanghai, China). SBP and DBP were measured in each group at a fixed time of 14:00 every week, from the day before the experiment to the 28 d after Ang II infusion. All measurements were performed by the same person at the same time of day. Before the measurement, mice were kept in the room quiet for 30 min, and the O-Cuff sensor and VPR sensor were put on the tail of the mice. SBP and DBP were measured three times for each mouse, and an average

was obtained. The mean arterial pressure (MAP) was calculated using the formula MAP = (SBP + DBP×2)/3.

Body Weight Measurement

On the 28th day of the experiment, after 12 h of fasting, the mice were weighed and then anesthesized with 1% pentobarbital sodium by intraperitoneal injection and sacrificed. The kidney was isolated and weighed to calculate the renal hypertrophy index using the following formula: Renal hypertrophy index (mg/g) = kidney weight (mg)/body weight (g).

Renal Function Analysis

Mice blood samples were collected via the tail vein on the 28th day of the experiment. Then, the serum was separated by centrifugation at 3000 g for 15 min. An automatic biochemical analyzer determined the serum creatinine (SCr), urea nitrogen (BUN), and cystatin C (Cys-C) levels.

Histology

Hematoxylin/eosin (HE) staining was applied to evaluate the degrees of renal fibrosis. For paraffin sections, kidney tissue was routinely prepared for embedding in paraffin and then post-fixed overnight in 4% paraformaldehyde. Sections were cut to a thickness of 4 μm and immediately placed on organosilane-coated slides. 4% paraformaldehyde was used overnight to post-fix the tissues. The following 24 hours were spent incubated in PBS that had been adjusted with three different buffers to a pH of 7.4 and 10% sucrose. The slices were then stained with HE following rehydration and deparaffinization in xylene. The fibrosis quantification was calculated by the ratio of fibrotic area to total area (collagen volume fraction).

Reactive Oxygen Species (ROS) Level Evaluation

Dihydroethidium (DHE, S0063; Beyotime) was employed as directed by the manufacturer to evaluate ROS generation in kidney tissues. Kidney tissues were incubated in 2.5 μM DHE for 30 minutes at 37°C in a dark place and then washed three times with PBS solution. A fluorescence microscope (Olympus Corporation) was used to detect the fluorescence.

Oxidative Stress Measurement

To obtain cell lysate, the kidney tissues were homogenized. The cell lysate was then stored at −80°C in the refrigerator. A commercial kit was used to measure the MDA (S0131S, Beyotime, Shanghai, China), SOD (S0109, Beyotime), CAT (S0051, Beyotime), and GSH-Px (S0056, Beyotime) activities, and a previously published protocol was followed to estimate the amount of oxidative stress.[23]

Enzyme-Linked Immunosorbent Assay (ELISA)

Serum and kidney tissue were collected from mice on day 28 after Ang II infusion. ELISA measured the concentrations of Ang II (E-EL-M2612c, Elabscience Biotechnology Co, Ltd) in serum and kidney lysate.

Cell Culture

Conditionally immortalized mouse podocytes (MPC5) were acquired from the Peking Union Medical College Cell Resource Center (PUMC) and were treated with recombinant IFN-γ containing 10% fetal bovine serum (FBS) and 10 U/mL. All cells in DMEM media were kept at 37°C, 5% CO_2 incubator. After passage, the cells were treated with 10% FBS but no IFN- γ. The cultured cells were induced to differentiate for two weeks in a 37°C, 5% CO_2 incubator.

Experimental Grouping

MPC5 were cultured in vitro and divided into four groups: (1) Control group: Low glucose DMEM medium; (2) SAL group: cells were treated with salidroside (10 μM); (3) Ang II group: cells were treated with Ang II (1 μM); (4) Ang II + SAL group: cells were treated with Ang II and SAL. Cells were incubated at 37°C for 24 h. Cells were incubated for the pathway inhibition experiment with Wnt/β-catenin pathway inhibitor ICG-001 (10 μM; HY-14428, MedChemExpress).

MTT Assay

In 96 well plates (1×10^3 cells/well), cells were seeded and incubated with or without inhibitor. After 48 hours, the cells were incubated for 4 hours at 37°C with 20 μL of MTT (M1020, Solarbio, Beijing, China). The absorbance at 570 nm was measured after adding 200 μL DMSO to determine the number of cells.

Cell Apoptosis Assay

Cell apoptosis was identified according to earlier study methods.[24] The Annexin V-FITC Apoptosis Detection Kit (CA1020, Beijing Solarbio Science & Technology Co, Ltd, China) was used to determine cell apoptosis. The cells were separated with trypsin-EDTA and collected by centrifugation.

The cells were washed with PBS saline before being suspended in a binding buffer and centrifuged at 300 g for 10 minutes. After exhausting the supernatant, the cells were arrested in a binding buffer containing 1×10^6 cells/mL. PI (5 μL) was added to the cells for 5 minutes under identical circumstances. A flow cytometer (Beckman Coulter, Inc, Brea, CA, USA) was used to assess apoptosis.

Quantitative Reverse Transcription Polymerase Chain Reaction (RT-qPCR)

TRizol (Invitrogen, USA) isolated total RNA from kidney tissues. Reverse transcription created complementary DNA (cDNA) from total RNA. To amplify the mRNA by Real-Time Quantitative PCR (RT-qPCR), SYBR Green reagent (TaKaRa, Japan) was used in an ABI Prism 7700 Real-Time PCR apparatus (Applied Biosystems, USA). Using the $2^{-\Delta\Delta Ct}$ formula, the relative gene expression was normalised to the internal control, GADPH.[25] The primers for Mouse Collagen I, Mouse Collagen III, Mouse α-SMA, Mouse AT1R, and Mouse GAPDH were designed by the NCBI Primer-Blast Tool (https://www.ncbi.nlm.nih. gov/tools/primer-blast/), which is listed in Table 1.

Western Blotting

The protein samples were collected after the cells were lysed using RIPA lysis buffer (Beyotime Biotechnology, Shanghai, China). A BCA kit (Beyotime) was used to determine protein concentration, and the equivalent volume of protein (40 μg for each well) was added and mixed with loading buffer (Beyotime) in a boiling-water bath for 3 minutes of denaturation. Once bromphenol blue reached the separation gel, electrophoresis was started for 30 minutes at 80 V and subsequently for 1∼2 hours at 120 V. The proteins were later placed onto membranes in an ice bath at 300 mA for 60 minutes. After rinsing the membranes for 1∼2 minutes with washing solution, they were inactivated for 1 hour at room temperature or sealed overnight at 4°C. The membranes received treatment with the primary antibodies against AT1R (1:500, ab124734, rabbit monoclonal, Abcam), Wnt1 (1:500, ab15251, rabbit polyclonal, Abcam), Wnt3a (1:500, ab219412, rabbit monoclonal, Abcam), β-Catenin (1:500, ab3257, rabbit monoclonal, Abcam), Beclin1 (1:500, sc-48341, mouse

Table 1. The Nucleotide Primer Sequences Used in This Study.

Genes	GenBank Accession No.	Forward Primer (5′-3′)	Reverse Primer (5′-3′)	Annealing Temperature (°C)	Amplicon Size (bp)
Mouse collagen I	NM_007742.4	GCTCCTCTTAGGGGCCACT	CCACGTCTCACCATTGGGG	55	103bp
Mouse collagen III	NM_009930.2	TCCCCTGGAATCTGTGAATC	TGAGTCGAATTGGGGAGAAT	52	63bp
Mouse α-SMA	NM_007392.3	TCCTGACGCTGAAGTATCCGATA	GGCCACACGAAGCTCGTTAT	55	101bp
Mouse AT1R	NM_177322.3	TTGTCCACCCGATGAAGTCTC	AAAAGCGCAAACAGTGATATTGG	54	158bp
Mouse GAPDH	NM_001411843.1	ACTCCACTCACGGCAAATTC	TCTCCATGGTGGTGAAGACA	52	171bp

monoclonal, Santa Cruz), p62 (1:500, ab56416, mouse monoclonal, Abcam), and GAPDH (1:2000, ab9485, rabbit polyclonal, Abcam) on a shaking table for 1 hour at room temperature. The membranes were washed with washing solution three times in 10 minutes before and after 1 hour of incubation with the secondary antibody at room temperature. After adding membranes to the developing liquid, chemiluminescence imaging analysis equipment (Gel Doc XR, Biorad) was used for observation.

Statistical Analysis

The mean ± standard deviation (SD) of at least three distinct experiments was used to express all data. Statistical analyses have been performed using SPSS 20.0 (SPSS, Chicago, IL, USA) or GraphPad Prism 9.0 software. The differences between several groups were examined using one-way ANOVA and the post hoc Tukey test. AF incidence between various groups was analyzed using Fisher's exact test. Statistical significance has been deemed as a P-value of <0.05.

Results

SAL Decreases Blood Pressure and Renal Hypertrophy Index in Ang II-Infused Mice

This experiment aimed to investigate the effects of SAL on blood pressure and renal hypertrophy index. Mice were used and infused with Ang II (2.0 mg/kg/day) or the same volume of saline using osmotic mini-pumps for 28 consecutive days. For 28 days, mice were given SAL (50 mg/kg/day, HY-N0109, MedChemExpress) or the same volume of saline before the start of Ang II infusion.

After 28 days of SAL administration, the in vivo systemic toxicity of SAL was evaluated. The mice's blood pressure and renal hypertrophy index were investigated. The results indicated that Ang II infusion led to an elevation in systolic blood pressure (SBP), diastolic blood pressure (DBP), and mean arterial blood pressure (MAP) in mice. However, treatment with SAL showed a reduction in these values (all, $P < 0.001$) (Figure 1(C)-(E)). Additionally, SAL pre-treatment increased body weight (BW) while decreasing kidney weight (KW) and renal hypertrophy index (KW/BW) in Ang II-infused mice (all, $P < 0.001$) (Figure 1(F)-(H)).

SAL Improves the Renal Function of Ang II-Infused Mice

To evaluate the effect of SAL on renal function, mice were subcutaneously infused with Ang II (2.0 mg/kg/day) or the same volume saline using osmotic mini-pumps for 28 days and intraperitoneally injected with salidroside (50 mg/kg/day) or the same volume saline two hours before the start of Ang II infusion. After 28 days of SAL administration, the renal function of mice was investigated. The histological analysis of renal tissues showed that SAL pre-treatment improved the renal function of mice (Figure 2A). Moreover, SAL pre-treatment significantly inhibited the serum creatinine (Scr), blood urea nitrogen (BUN), and serum cystatin C (Cys-C) levels (all, $P < 0.001$), which were increased by Ang II-induced (Figure 2(B)-(D)). The findings suggest that SAL pre-treatment improved the renal function of mice infused with Ang II.

SAL Attenuates Renal Fibrosis and Related Molecule Expression in Ang II-Infused Mice

To study the effect of SAL on Ang II-induced renal fibrosis and molecule expression, mice were subcutaneously infused with Ang II (2.0 mg/kg/day) and intraperitoneally injected with SAL (50 mg/kg/day) or the same volume saline 2 h before the start of Ang II infusion. Ang II significantly increased the renal fibrotic area, while SAL remarkably attenuated this effect (Figure 3(A) and (B)). RT-qPCR was performed to measure the mRNA expression of several fibrotic markers, including Collagen I, Collagen III, and α-smooth muscle actin (α-SMA). The results demonstrated that SAL inhibited the expression of Collagen I, Collagen III, and α-SMA (all, $P < 0.001$) (Figure 3(C)).

SAL Attenuates Ang II-Induced Oxidative Stress in Renal Tissue of Mice

The key biomarkers of oxidative stress, including malondialdehyde (MDA), superoxide dismutase (SOD), catalase (CAT), and glutathione peroxidase (GSH-Px) were determined in the lysate of renal tissue. The formation of reactive oxygen species (ROS) in the renal tissue was significantly enhanced following Ang II therapy, as seen by DHE staining (Figure 4(A)). Additionally, compared to the Ang II group, the DHE-positive cells were considerably reduced after pre-treatment with SAL ($P < 0.001$) (Figure 4(B)). Ang II infusion increased levels of MDA content and decreased SOD, CAT, and GSH-Px activities. At the same time, these changes were all reversed by SAL pre-treatment (all, $P < 0.001$) (Figure 4(C)-(F)).

SAL Inhibits the Expression of AT1R and Key Factors of the Wnt/β-Catenin Pathway in Ang II-Treated Mice

We measured the serum Ang II protein levels and Ang II levels in kidney tissues of Ang II-infused mice by ELISA and mRNA expression of AT1R in renal tissues via RT-qPCR. The results showed that Ang II infusion stimulated the expression of serum Ang II protein levels, Ang II levels in kidney tissues, and expression of AT1R in renal tissues. At the same time, SAL pre-treatment did not affect the expression of serum Ang II protein and Ang II in kidney tissue levels but significantly inhibited AT1R expression in renal tissues ($P < 0.001$) (Figure 5(A)-(C)). In addition, the Western blot was used to measure the protein level of critical factors of the Wnt/β-catenin pathway. The
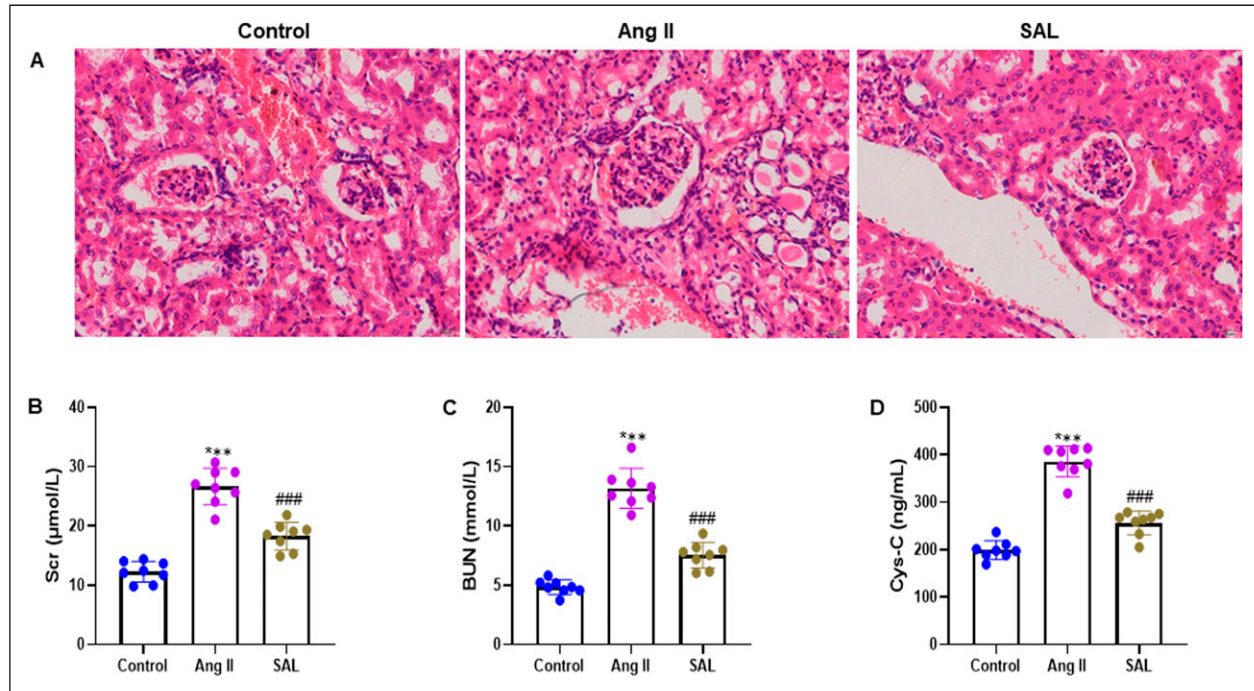
Figure 2. SAL improves the renal function of Ang II-infused mice. (A) The histological changes of the renal tissues by HE staining (400×). (B) Serum creatinine (Scr), (C) Blood urea nitrogen (BUN), and (D) serum cystatin C (Cys-C) were determined in mice of each group. Data are presented as mean ± SD (n = 8 in each group). ***$P < 0.001$ vs control group; ###$P < 0.001$ vs Ang II group.
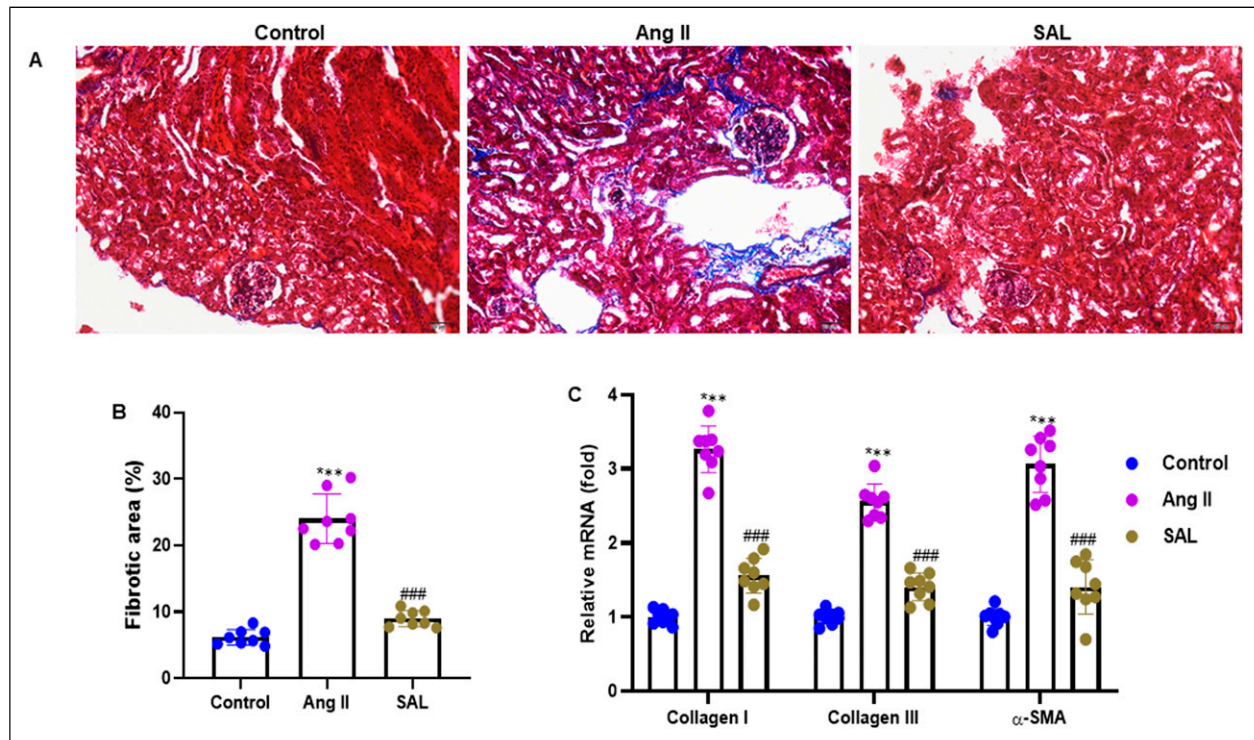

Figure 3. SAL suppresses renal fibrosis and the expression of related molecules in Ang II-infused mice. (A) Paraffin-embedded kidney sections (4-μm thickness) were stained with Masson trichrome (Magnification ×200). (B) The fibrosis area was calculated to assess the extent of kidney fibrosis. (C) RT-qPCR was performed to determine the mRNA expression of three fibrosis-related genes: Collagen I (COL1A1), Collagen III (COL3A1) and α-SMA. Data are presented as mean ± SD (n = 8 in each group). ***$P < 0.001$ vs control group; ###$P < 0.001$ vs Ang II group. α-SMA; α-smooth muscle actin.
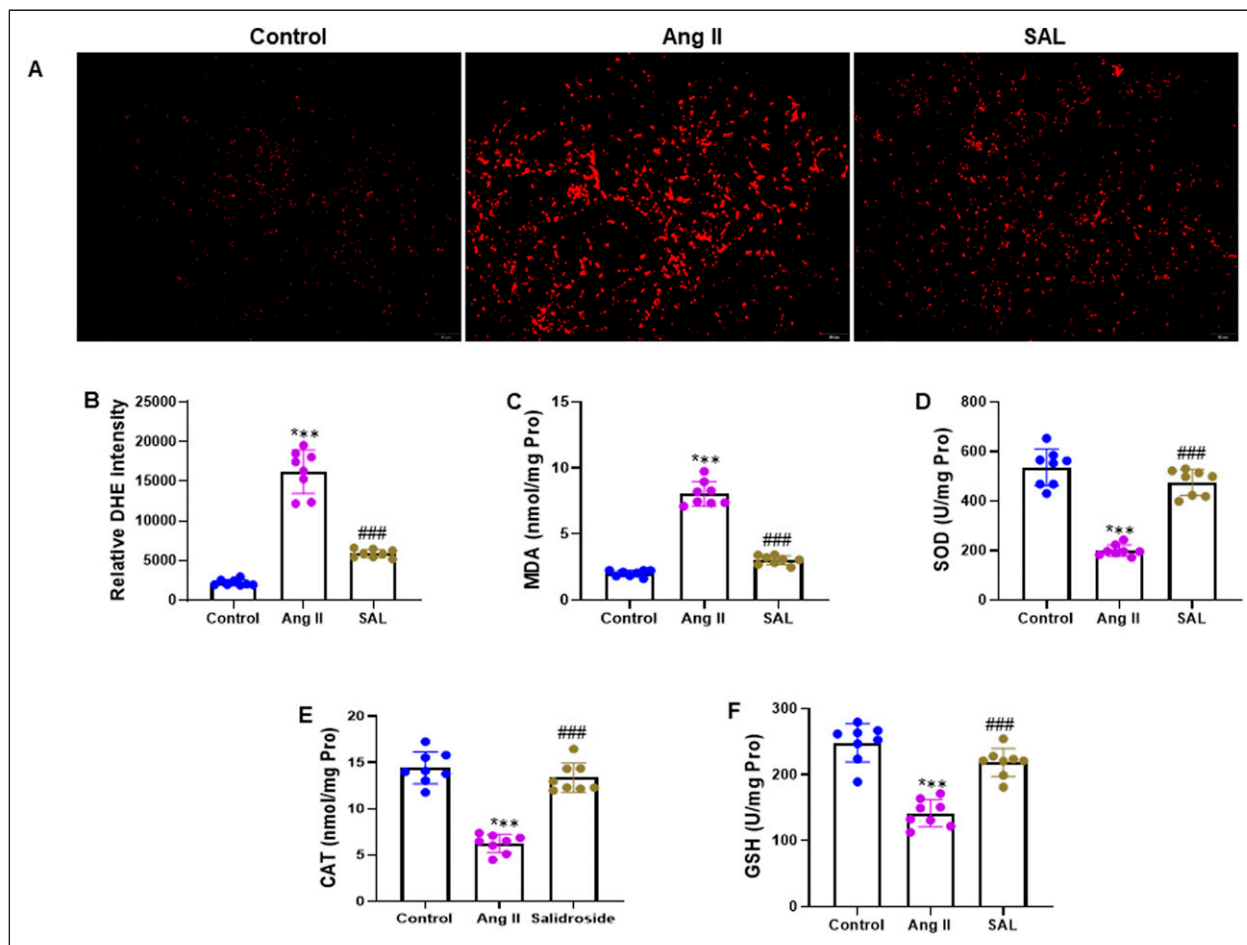
Figure 4. SAL suppresses oxidative stress in renal tissue of mice with Ang II infusion. (A) Paraffin-embedded kidney sections were stained with DHE (200×). (B) Quantification of relative DHE intensity. The kidney tissue lysate was analyzed for (C) MDA, (D) SOD, (E) CAT and (F) GSH-Px. Data are presented as mean ± SD (n = 8 in each group). ***$P < 0.001$ vs control group; ###$P < 0.001$ vs Ang II group. DHE, dihydroethidium; MDA, malondialdehyde; SOD, superoxide dismutase; CAT, catalase; GSH-Px, glutathione peroxidase.

results demonstrated that SAL pre-treatment inhibited AT1R, Wnt1, Wnt3a, and β-catenin expressions (all, $P < 0.001$) (Figure 5(D) and (E), Fig. S1). Protein expression was normalized to the expression of GAPDH.

SAL Suppresses Ang II-Induced Podocyte Injury and Regulates AT1R and β-Catenin Protein Expression

MPC5 were pretreated with SAL (10 μM) for 2 hours, then incubated with Ang II (1 μM) for an additional 24 hours, and cell viability was determined using an MTT examination. The results showed that Ang II incubation reduced the cell viability rate. At the same time, Ang II + SAL pre-treatment improved the cell viability rate (Figure 6(A)). Ang II + SAL pre-treatment also suppressed Ang II-induced podocyte apoptosis rate (Figure 6(B) and (C)). To investigate the expression of AT1R and β-catenin proteins, we performed the western blot analysis and quantified the proteins' band intensity. The results showed

that Ang II decreased the expression of AT1R protein and increased the expression of Wnt1, Wnt3, and β-catenin proteins. However, treatment with Ang II + SAL increased the expression of AT1R protein while reducing the expression of Wnt1, Wnt3, and β-catenin proteins (all, $P < 0.001$) (Figure 6(D) and (E), Fig. S2). Thus, the results showed SAL protects podocyte cells against Ang II-induced injury and regulates the AT1R and β-catenin protein expression.

SAL Attenuates Intracellular ROS Generation and Oxidative Stress in Ang II-Treated Podocytes

MPC5 were pretreated with SAL (10 μM) or Wnt/β-catenin pathway inhibitor ICG-001 (10 μM) for 2 h, followed by incubation with Ang II (1 μM) for a further 24 h. Podocyte cells were stained with DHE to assess the intracellular ROS level, and the intracellular ROS was quantified by calculating the percentage of DHE + cells. The results showed that
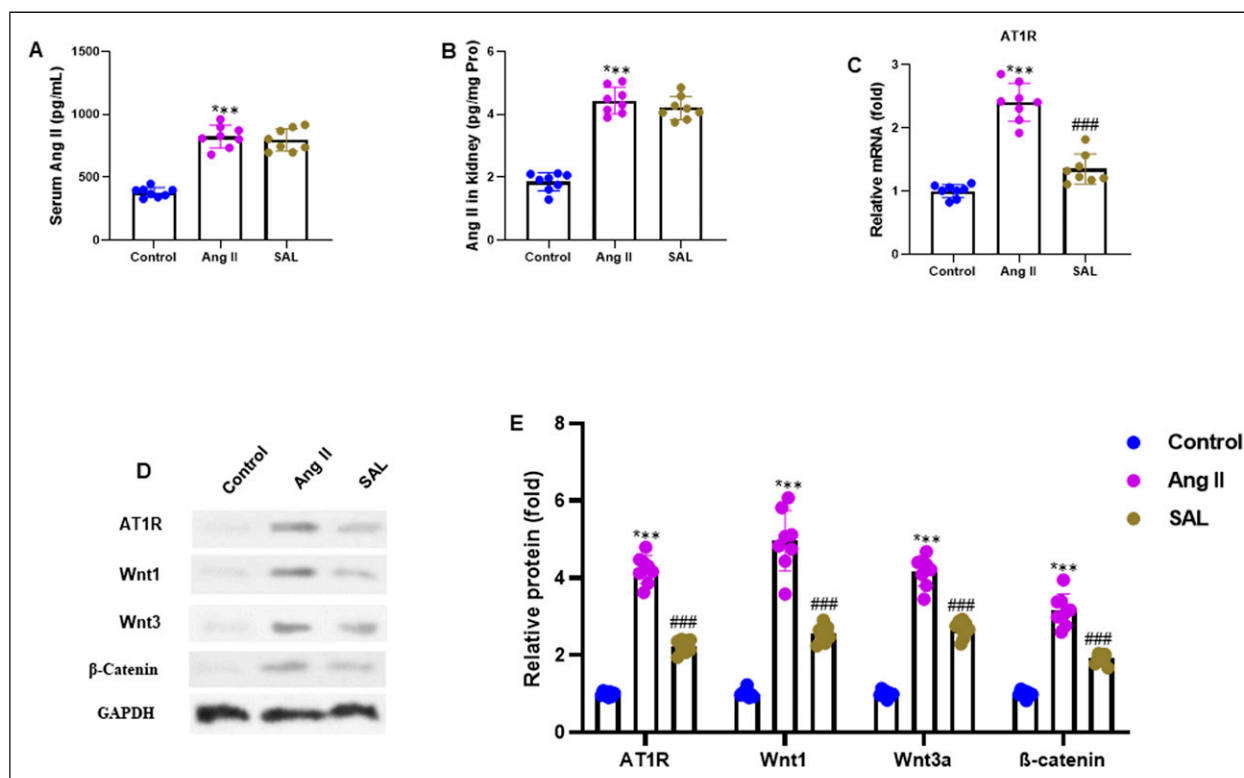
Figure 5. SAL suppressed the expression of AT1R and key factors of the Wnt/β-catenin pathway in Ang II-treated mice. (A) ELISA measured serum Ang II protein levels in mice infused with Ang II. (B) ELISA measured Ang II levels in kidney tissues of Ang II-infused mice (data are normalized to total proteins). (C) RT-qPCR measured the mRNA expression of AT1R in mouse kidney tissues. (D) The protein expression was measured by Western blot, and the representative bands are shown. (E) Quantification of protein bands of AT1R, Wnt1, Wnt3a, and β-catenin. Protein expression was normalized to the expression of GAPDH. Data are presented as mean ± SD (n = 8 in each group). ***$P < 0.001$ vs control group; ###$P < 0.001$ vs Ang II group. AT1R, Ang II type 1 receptor.

podocyte incubation with Ang II stimulated the ROS level, which was inhibited by Ang II + SAL and Ang II + ICG-001 ($P < 0.001$) (Figure 7(A) and (B)). Moreover, the oxidative stress marker genes were detected in the cell culture supernatant of podocytes. The results indicated that incubation with Ang II increased the MDA level while decreasing the SOD and CAT levels. However, Ang II + SAL and Ang II + ICG-001 treatments observed the reverse expression patterns (all, $P < 0.001$) (Figure 7(C) and (D)). Therefore, the results demonstrated that SAL inhibits intracellular ROS levels and oxidative stress in Ang II-treated podocytes.

SAL Inhibits Autophagy in Ang II-Treated Podocytes

Podocytes were stained with LC3-II and DAPI fluorescence. The nuclei of surviving cells were stained with DAPI and showed blue fluorescence. The cytoplasm of autophagy cells is stained with LC3-II and shows green fluorescence. We also quantitatively analyzed the proportion of autophagy cells in each group. We observed a high proportion of autophagy cells in the Ang II group compared with the control group. Meanwhile, SAL and ICG-001 treatments decreased the proportion of autophagy cells in the Ang II + SAL and Ang II + ICG-001

groups (all, $P < 0.001$) (Figure 8(A) and (B)). We performed the western blot analysis to investigate the expression of autophagy-related proteins such as Beclin1 and p62 and quantified the proteins' band intensity. The results showed that the Ang II + SAL and Ang II + ICG-001 treatments reduced the Beclin1 protein expression, whereas they enhanced the p62 protein expression (all, $P < 0.001$) (Figure 8(C) and (D), Fig. S3). Therefore, the results demonstrated that SAL pre-treatment attenuates the autophagy in Ang II-treated podocyte cells.

Discussion

The current study demonstrated how SAL affected hypertensive renal injury and fibrosis. Our data showed that SAL significantly attenuated the blood pressure and renal hypertrophy index in Ang II-infused mice. SAL pre-treatment improved the renal function of Ang II-treated mice. SAL significantly inhibited renal fibrosis and the expression of Collagen I, Collagen III, and α-SMA. In addition, SAL reduced the Ang II-induced oxidative stress in the renal tissue of mice. Further, SAL inhibited the expression of AT1R and critical factors of the Wnt/β-catenin pathway in vivo. Thus, the
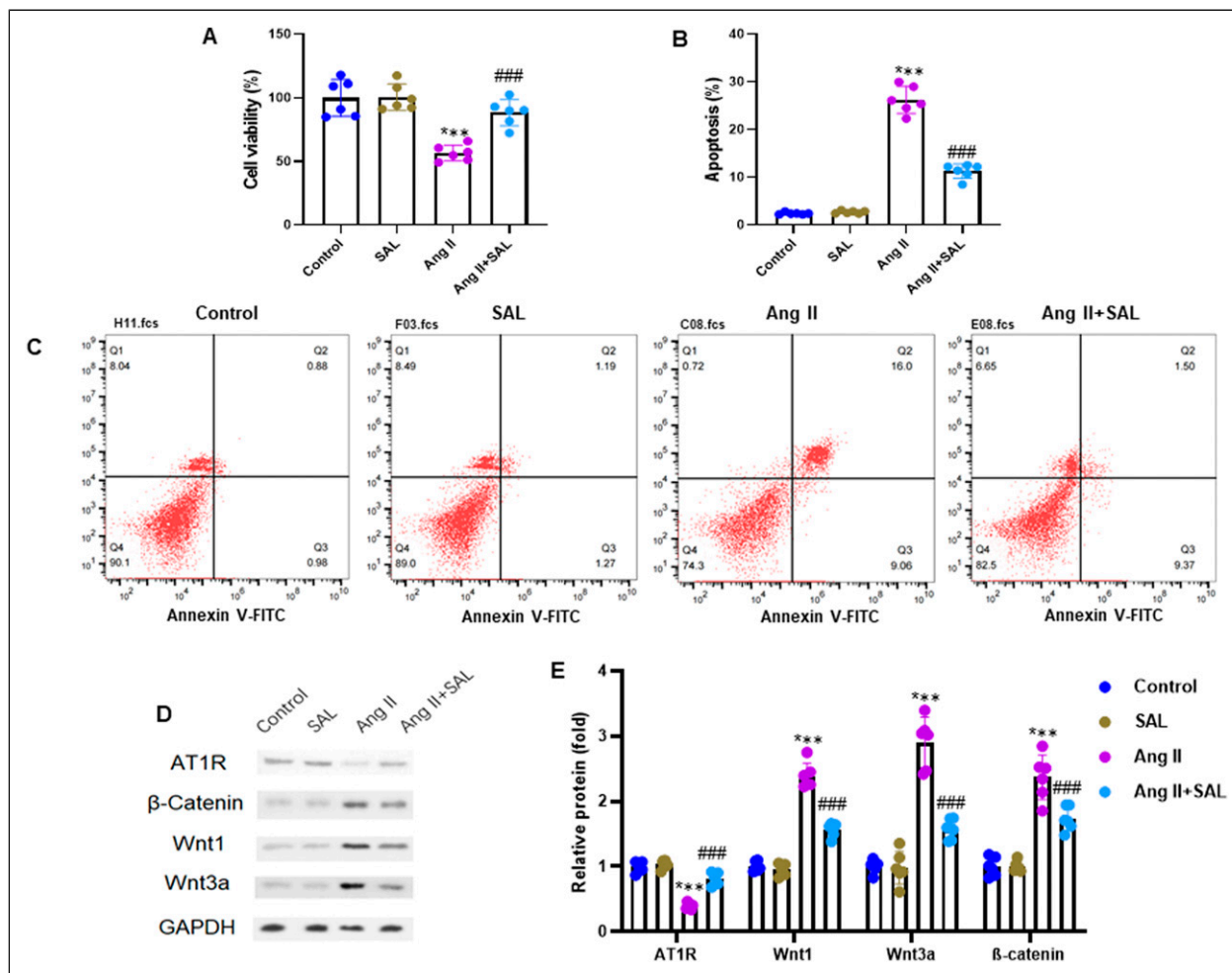
Figure 6. SAL suppresses Ang II-induced podocyte injury and modulates AT1R and β-catenin protein expression. MPC5 mouse renal podocytes were pretreated with SAL (10 μM) for 2 h, followed by incubation with Ang II (1 μM) for a further 24 h, and an MTT assay was used to measure cell viability. (B) SAL attenuated Ang II-induced podocyte apoptosis rate. (C) Representative image of apoptosis that was determined by flow cytometry. (D) The protein expression was measured by Western blot, and the representative bands are shown. (E) Quantification of protein bands of AT1R, Wnt1, Wnt3a, and β-catenin. GAPDH expression was used to normalize protein expression. Data are presented as mean ± SD (n = 6 in each group). ***$P < 0.001$ vs control group; ###$P < 0.001$ vs Ang II group.

results showed that SAL could have a significant therapeutic impact on hypertensive renal injury and fibrosis.

A Previous study reported that Rhodiola's important metabolites include phenylethanol derivatives, monoterpenes, triterpenes, flavonoids, and phenolic acids.[26] The U.S. Food and Drug Administration (FDA) has issued warning letters to rhodiola supplement producers regarding purity, health claims and branding as drugs.[27] However, SAL has been shown to have a significant hypoglycemic impact on diabetes[28] as well as a positive effect on diabetic vascular disorders.[29] Also, SAL has been shown to affect lipid metabolism in type 2 diabetic mice by down-regulating miR-370 in primary hepatocytes.[30] In this study, intraperitoneally injection of 50 mg/kg/day SAL significantly reduced blood pressure, consistent with the earlier study.[31] Furthermore, our data indicated that pre-treatment with SAL increased body weight (BW) while

decreasing kidney weight (KW) and the renal hypertrophy index (KW/BW) in Ang II-infused mice.

Acute kidney injury (AKI) is a well-known clinical condition characterized by an immediate decrease in renal function that leads to multiorgan failure in critically sick individuals. AKI is associated with several renal disorders.[32] A recent study reported that LPS-treated mice developed severe renal pathology, including tubular cell vacuolation, glomerular atrophy, tubular cell necrosis, tubular dilatation and distortion, and nuclear loss. An increase in Scr and BUN levels accompanied these changes, and SAL pre-treatment reduced the Scr and BUN levels in mice with AKI.[33] However, the renal functions of all groups were evaluated by assessing the levels of serum creatinine (Scr), blood urea nitrogen (BUN), and serum cystatin C (Cys-C) and observing renal histopathological sections stained in Ang II-infused mice. The data showed
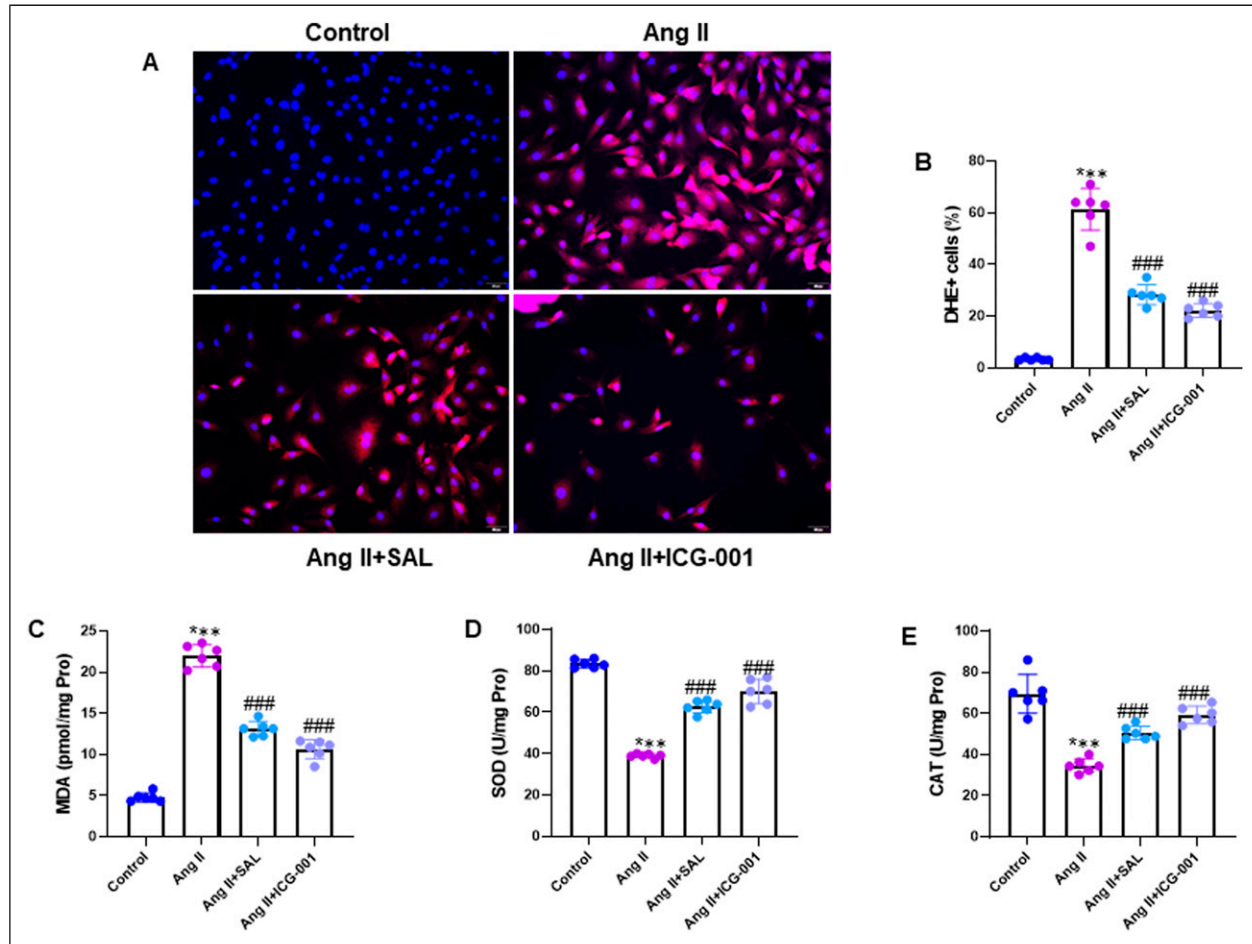
Figure 7. SAL inhibits Ang II-induced intracellular ROS generation and oxidative stress via the Wnt/β-catenin pathway. MPC5 podocytes were pretreated with SAL (10 μM) or Wnt/β-catenin pathway inhibitor ICG-001 (10 μM) for 2 h, followed by incubation with Ang II (1 μM) for a further 24 h. (A) Podocytes were stained with DHE to assess the intracellular ROS level and photographed in the fluorescence microscope (200×). (B) Quantification of intracellular ROS by calculating the percentage of DHE + cells. The oxidative stress indicators were detected in cell culture supernatant of podocytes: (C) MDA, (D) SOD and (E) CAT. Data are shown as mean ± SD (n = 6 per group). DHE, dihydroethidium. ***$P < 0.001$ vs control group; ###$P < 0.001$ vs Ang II group.

that pre-treatment with SAL significantly decreased the Scr, BUN, and Cys-C levels, which had increased due to Ang II infusion. The results suggest that SAL pre-treatment improved the renal function of Ang II-infused mice.

Considering most renal illnesses lead to renal fibrosis, there is a significant interest in finding the underlying causes of this disorder to avert or reverse renal fibrosis. Excess extracellular matrix deposition and renal fibrosis result from the proliferation of interstitial fibroblasts with myofibroblast transformation.[34] An excess of ECM, such as collagen I, collagen III, and fibronectin, characterizes most chronic kidney diseases (CKDs).[35] Many cells in the tubulointerstitium of the kidneys can produce ECM, and fibroblasts are the primary matrix-producing cells that generate many interstitial matrix components. Kidney fibroblasts are distinct, including SMA-positive myofibroblasts.[36] In the present study, we investigated the impact of SAL on renal fibrosis by examining its effects on Ang II-infused mice. Our findings showed that SAL significantly inhibited the expression of

Collagen I, Collagen III, and α-SMA. Therefore, our research demonstrates that SAL can potentially decreased renal fibrosis and related molecule expression in the presence of Ang II treatment.

Most aerobic organisms generate reactive oxygen species (ROS), and the concentration of ROS regulates their biological activity. Under standard settings, low ROS concentrations are unavoidable in physiological activities. During pathological conditions, however, substantial quantities of ROS are generated.[37] High amounts of ROS can degrade cellular macromolecules such as proteins, lipids, and nucleic acids, resulting in cellular damage.[37] Aerobic organisms have evolved an adequate antioxidant defence system to defend themselves from ROS-induced cellular damage.[38] The current study showed that the Ang II group had higher MDA concentration and lower SOD protein expression in renal tissue compared with the control group. These data suggest that high ROS levels during renal damage depleted antioxidant enzymes. Additionally, SOD expression was enhanced by SAL cotreatment, leading to a
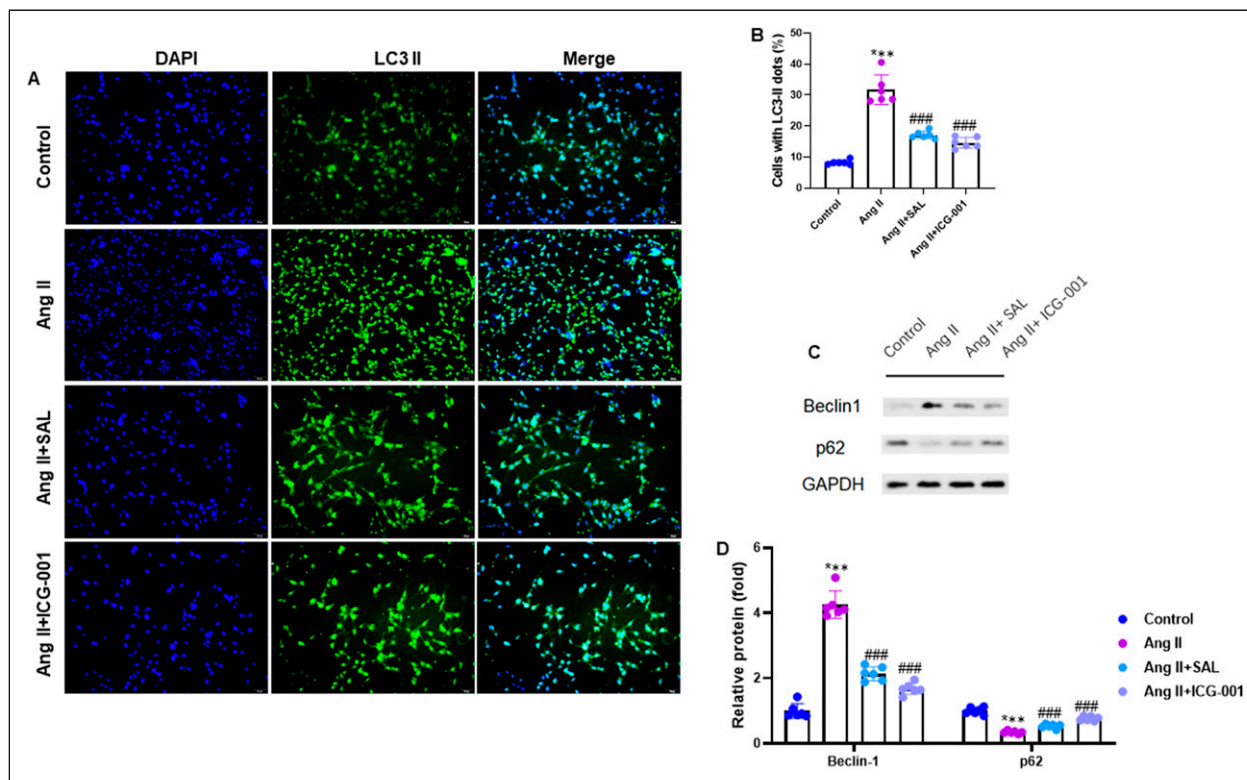
Figure 8. SAL inhibits Ang II-induced autophagy via the Wnt/β-catenin pathway. (A) Podocytes were stained with LC3-II and DAPI fluorescence. The nuclei of surviving cells were stained with DAPI and showed blue fluorescence; The cytoplasm of autophagic cells was stained with LC3-II and showed green fluorescence (200×). (B) Quantitative analysis of the proportion of autophagic cells in each group. (C) The autophagy-related protein expression was measured by Western blot, and the representative bands are shown. (D) Quantification of protein bands of Beclin1 and p62. Protein expression was normalized to the expression of GAPDH. Data are shown as mean ± SD (n = 6 per group). ***P < 0.001 vs control group; ###P < 0.001 vs Ang II group.

significant reduction in MDA levels in the Ang II group. These findings indicate that SAL cotreatment decreased ROS levels by increasing SOD protein expression.

SAL is a potent antioxidant found to reduce oxidative stress in diabetic mice.[27] A study by Zhang et al[39] showed that salidroside, a compound found in SAL, protected neuronal cells from hydrogen peroxide toxicity by up-regulating antioxidant genes such as HO-1 and peroxiredoxin 1 and anti-apoptotic genes. In another study, Langer et al[40] found that metformin, a drug used to treat diabetes, had an antioxidant effect that reduced cell apoptosis. Our research supports these findings, as SAL pre-treatment protected podocyte cells from apoptosis caused by Ang II treatment.

One of the critical signaling mechanisms leading to kidney disease is the Wnt/β-catenin pathway. A growing number of studies have shown that stimulation of the Wnt/β-catenin signaling pathway plays a vital role in developing renal fibrosis by modulating the expression of several downstream mediators involved in renal fibrosis.[41-43] Transient activation of different signaling pathways promotes the regeneration of damaged tissues. However, their persistent stimulation causes fibrosis.[44] It has been demonstrated that severe ischemia/reperfusion damage causes prolonged and excessive

production of Wnt/β-catenin, which is followed by interstitial myofibroblast activation and ECM deposition, which are hallmarks of the development of renal fibrotic lesions.[45] Our study found that pre-treatment with SAL played a crucial role in reducing the expression of AT1R, Wnt1, Wnt3a, and β-catenin proteins in mice with hypertensive renal injury and fibrosis caused by Ang II infusion and IFN-γ-stimulated podocytes. These results highlight the potential of SAL in decreasing hypertensive renal injury and fibrosis induced by Ang II by inhibiting the Wnt/β-catenin pathway.

Limitations

Our study has several limitations that need to be mentioned. Firstly, a power calculation was not conducted to determine the requisite sample size for the study. In future research, we will perform a power calculation to identify the suitable sample size. Secondly, we did not examine the effectiveness of the SAL in a dose-dependent manner. Thirdly, female mice were not included in the in vivo tests to investigate the underlying mechanism of SAL's protective effect against Ang II-induced hypertensive renal damage and fibrosis. Fourthly, the underlying findings of

the study have not been independently confirmed in pre-clinical or clinical settings. Fifthly, more investigation is needed to determine the underlying mechanism of SAL's preventive impact against Ang II-induced hypertensive renal injury and fibrosis. Despite these limitations, our study provides significant evidence of SAL's protective effects against hypertensive renal injury and fibrosis, both in vivo and in vitro.

Conclusion

In the present research, we investigated the possible protective impact of SAL on Ang II-induced hypertensive renal injury and fibrosis in vivo and in vitro. Our results indicate that SAL pre-treatment inhibited Ang II-induced hypertensive renal injury and fibrosis by downregulating the Wnt/β-catenin pathway. Future research could validate these results in pre-clinical and clinical contexts.

Author Contributions

All authors significantly contributed in this study. **Jie Zhu** and **Liang Li** performed experiments and wrote the manuscript; **Yuting Luan** and **Ziqing Zhang** performed experiments, revised the manuscript, and provided statistical analysis; **Yi Wang** and **Zhenyu Xu** conceived the idea, designed and supervised the study.

Declaration of Conflicting Interests

The author(s) declared no potential conflicts of interest with respect to the research, authorship, and/or publication of this article.

Ethical Statement

Ethics Approval and Consent to Participate

This study was approved (**2021-7th-HIRB-029**) by Seventh People's Hospital of Shanghai University of Traditional Chinese Medicine Ethics Committee. The authors envisaged all standard protocols in accordance with the 1964 Declaration of Helsinki. All methods carried out in this study were in accordance with ARRIVE guidelines.

Consent for Publication

All authors were agreed to publish this research work.

ORCID iD

Zhenyu Xu https://orcid.org/0000-0003-0942-5139

Data Availability Statement

Due to confidential issues, the datasets generated and/or analyzed during the current work are not publicly available but are available from the corresponding author upon reasonable request.

Supplemental Material

Supplemental material for this article is available online.

References

1. Aibara Y, Nakashima A, Kawano KI, et al. Daily low-intensity pulsed ultrasound ameliorates renal fibrosis and inflammation in experimental hypertensive and diabetic nephropathy. *Hypertension*. 2020;76:1906-1914.
2. Tao M, Shi Y, Tang L, et al. Blockade of ERK1/2 by U0126 alleviates uric acid-induced EMT and tubular cell injury in rats with hyperuricemic nephropathy. *Am J Physiol Ren Physiol*. 2019;316:F660-F673.
3. François H, Placier S, Flamant M, et al. Prevention of renal vascular and glomerular fibrosis by epidermal growth factor receptor inhibition. *Faseb J*. 2004;18:926-928.
4. Epstein M, Kovesdy CP, Clase CM, Sood MM, Pecoits-Filho R. Aldosterone, mineralocorticoid receptor activation, and CKD: a review of evolving treatment paradigms. *Am J Kidney Dis*. 2022; 80:658-666.
5. Manrique C, Lastra G, Gardner M, Sowers JR. The renin angiotensin aldosterone system in hypertension: roles of insulin resistance and oxidative stress. *Med Clin*. 2009;93: 569-582.
6. Lu Q, Ma Z, Ding Y, et al. Circulating miR-103a-3p contributes to angiotensin II-induced renal inflammation and fibrosis via a SNRK/NF-κB/p65 regulatory axis. *Nat Commun*. 2019;10: 2145.
7. Yoon JJ, Lee HK, Kim HY, et al. Sauchinone protects renal mesangial cell dysfunction against angiotensin II by improving renal fibrosis and inflammation. *Int J Mol Sci*. 2020;21:7003.
8. Zhang JH, Li J, Ye Y, Yu WQ. rAAV9-mediated supplementation of miR-29b improve angiotensin-II induced renal fibrosis in mice. *Mol Med*. 2021;27:89.
9. Zhang SF, Mao XJ, Jiang WM, Fang ZY. Qian yang yu yin granule protects against hypertension-induced renal injury by epigenetic mechanism linked to nicotinamide N-methyltransferase (NNMT) expression. *J Ethnopharmacol*. 2020;255:112738.
10. Panossian A, Wikman G, Sarris J. Rosenroot (Rhodiola rosea): traditional use, chemical composition, pharmacology and clinical efficacy. *Phytomedicine*. 2010;17:481-493.
11. Pu W, Zhang M, Bai R, et al. Anti-inflammatory effects of Rhodiola rosea L.: a review. *Biomed Pharmacother*. 2020;121: 109552.
12. Tao H, Wu X, Cao J, et al. Rhodiola species: a comprehensive review of traditional use, phytochemistry, pharmacology, toxicity, and clinical study. *Med Res Rev*. 2019;39:1779-1850.
13. Basnyat B, Murdoch DR. High-altitude illness. *Lancet*. 2003; 361:1967-1974.

14. Yu P, Hu C, Meehan EJ, Chen L. X-ray crystal structure and antioxidant activity of salidroside, a phenylethanoid glycoside. *Chem Biodivers*. 2007;4:508-513.

15. Tang H, Gao L, Mao J, et al. Salidroside protects against bleomycin-induced pulmonary fibrosis: activation of Nrf2-antioxidant signaling, and inhibition of NF-κB and TGF-β1/Smad-2/-3 pathways. *Cell Stress Chaperones*. 2016;21: 239-249.

16. Feng J, Chen K, Xia Y, et al. Salidroside ameliorates autophagy and activation of hepatic stellate cells in mice via NF-κB and TGF-β1/Smad3 pathways. *Drug Des Dev Ther*. 2018;12: 1837-1853.

17. Chen H, Lin Y, Zeng L, Liu S. Elucidating the mechanism of Hongjinshen decoction in the treatment of pulmonary fibrosis based on network pharmacology and molecular docking. *Medicine*. 2022;101:e32323.

18. Yang S, Pei T, Wang L, et al. Salidroside alleviates renal fibrosis in SAMP8 mice by inhibiting ferroptosis. *Molecules*. 2022;27: 8039.

19. MacDonald BT, Tamai K, He X. Wnt/beta-catenin signaling: components, mechanisms, and diseases. *Dev Cell*. 2009;17:9-26.

20. Xiao L, Wang M, Yang S, Liu F, Sun L. A glimpse of the pathogenetic mechanisms of Wnt/β-catenin signaling in diabetic nephropathy. *BioMed Res Int*. 2013;2013:987064.

21. Zhou D, Tan RJ, Fu H, Liu Y. Wnt/β-catenin signaling in kidney injury and repair: a double-edged sword. *Lab Invest*. 2016;96: 156-167.

22. Bose M, Almas S, Prabhakar S. Wnt signaling and podocyte dysfunction in diabetic nephropathy. *J Invest Med*. 2017;65: 1093-1101.

23. Ma JY, Zhang WX, Chen H, et al. The protective effects of echinacoside on oxidative stress injury in vascular dementia rats. *Chin Pharmacol Bull*. 2014; 30: 638-642.

24. Lim W, An Y, Yang C, Bazer FW, Song G. Chrysophanol induces cell death and inhibits invasiveness via mitochondrial calcium overload in ovarian cancer cells. *J Cell Biochem*. 2018; 119:10216-10227.

25. Pfaffl MW. A new mathematical model for relative quantification in real-time RT-PCR. *Nucleic Acids Res*. 2011;29:e45.

26. Sun AQ, Ju XL. Advances in research on anticancer properties of salidroside. *Chin J Integr Med*. 2021;27:153-160.

27. Warning letters. U.S. Food & drug administration.

28. Li F, Tang H, Xiao F, Gong J, Peng Y, Meng X. Protective effect of salidroside from rhodiolae radix on diabetes-induced oxidative stress in mice. *Molecules*. 2011;16:9912-9924.

29. Alameddine A, Fajloun Z, Bourreau J, et al. The cardiovascular effects of Salidroside in the Goto-Kakizaki diabetic rat model. *J Physiol Pharmacol*. 2016;66:249-257.

30. Zhang XR, Fu XJ, Zhu DS, et al. Salidroside-regulated lipid metabolism with down-regulation of miR-370 in type 2 diabetic mice. *Eur J Pharmacol*. 2016;779:46-52.

31. Ma YG, Wang JW, Bai YG, Liu M, Xie MJ, Dai ZJ. Salidroside contributes to reducing blood pressure and alleviating cerebrovascular contractile activity in diabetic Goto-Kakizaki Rats by inhibition of L-type calcium channel in smooth muscle cells. *BMC Pharmacol Toxicol*. 2017;18:30.

32. Schaalan MF, Mohamed WA. Determinants of hepcidin levels in sepsis-associated acute kidney injury: impact on pAKT/PTEN pathways? *J Immunot*. 2016;13:751-757.

33. Pan J, Zhu J, Li L, Zhang T, Xu Z. Salidroside attenuates LPS-induced kidney injury through activation of SIRT1/Nrf2 pathway. *Hum Exp Toxicol*. 2023;42:9603271231169520.

34. Liu Y. Cellular and molecular mechanisms of renal fibrosis. *Nat Rev Nephrol*. 2011;7:684-696.

35. Kuma A, Tamura M, Otsuji Y. Mechanism of and therapy for kidney fibrosis. *J UOEH*. 2016;38:25-34.

36. Böttinger EP. TGF-beta in renal injury and disease. *Semin Nephrol*. 2007;27:309-320.

37. Wei SM, Huang YM, Qin ZQ. Salidroside exerts beneficial effect on testicular ischemia-reperfusion injury in rats. *Oxid Med Cell Longev*. 2022;2022:8069152.

38. Filho DW, Torres MA, Bordin AL, Crezcynski-Pasa TB, Boveris A. Spermatic cord torsion, reactive oxygen and nitrogen species and ischemia-reperfusion injury. *Mol Aspect Med*. 2004;25:199-210.

39. Zhang L, Yu H, Sun Y, et al. Protective effects of salidroside on hydrogen peroxide-induced apoptosis in SH-SY5Y human neuroblastoma cells. *Eur J Pharmacol*. 2007;564:18-25.

40. Langer S, Kreutz R, Eisenreich AL. Metformin modulates apoptosis and cell signaling of human podocytes under high glucose conditions. *J Nephrol*. 2016;29:765-773.

41. Chen L, Chen DQ, Wang M, et al. Role of RAS/Wnt/β-catenin axis activation in the pathogenesis of podocyte injury and tubulo-interstitial nephropathy. *Chem Biol Interact*. 2017;273:56-72.

42. Feng YL, Chen DQ, Vaziri ND, Guo Y, Zhao YY. Small molecule inhibitors of epithelial-mesenchymal transition for the treatment of cancer and fibrosis. *Med Res Rev*. 2019;40:54-78.

43. Schunk SJ, Floege J, Fliser D, Speer T. WNT-β-catenin signalling -A versatile player in kidney injury and repair. *Nat Rev Nephrol*. 2020;17:172-184.

44. Edeling M, Ragi G, Huang S, Pavenstädt H, Susztak K. Developmental signalling pathways in renal fibrosis: the roles of notch, Wnt and hedgehog. *Nat Rev Nephrol*. 2016;12:426-439.

45. Xiao L, Zhou D, Tan RJ, et al. Sustained activation of wnt/β-catenin signaling drives AKI to CKD progression. *J Am Soc Nephrol*. 2016;27:1727-1740.